Strong-field phase-dependent molecular dissociation

Sarah R. Nichols and Thomas C. Weinacht*
Department of Physics, Stony Brook University, Stony Brook, New York 11794, USA

Tamás Rozgonyi
Institute of Structural Chemistry, Chemical Research Center of the HAS, Budapest 1525, Hungary

Brett J. Pearson
Department of Physics and Astronomy, Dickinson College, Carlisle, Pennsylvania 17013, USA
(Received 29 August 2008; published 7 April 2009)

We show how wave functions with the same energy and probability distribution but different momenta have very different dissociation probabilities when two molecular potentials are strongly coupled by an intense laser field. Our measurements of dynamics in a molecular family, in conjunction with molecular structure and wave-packet calculations, highlight the role of the wave-packet momentum, or spatially varying phase, in the dynamics leading to dissociation. Phase-dependent dynamics are central to coherent control of laser driven chemistry.

DOI: 10.1103/PhysRevA.79.043407 PACS number(s): 33.80.−b, 31.15.xv

I. INTRODUCTION

With the advent of ultrafast lasers, experimental measurements have been able to track the influence of coherent wave-packet motion during simple chemical reactions such as bond breaking before energy is statistically redistributed in the molecule [1]. In a typical pump-probe femtochemistry experiment, an ultrafast pump pulse excites a coherent superposition of vibrational eigenstates on a potential-energy surface, leading to time-dependent evolution of the nuclear coordinate expectation values. Varying the delay of a subsequent probe pulse can control the product yield by modifying the excitation probability to a final potential-energy surface where, in case of bond breaking, the wave packet moves toward dissociation. The timing of the probe pulse determines whether the wave packet is in the Franck-Condon (FC) region for transfer to the final state, and thus the experiment relies on the evolution of the probability density on the intermediate-state surface. The dissociation probability can be modulated by the coherent vibrational motion of the wave packet, but the reaction dynamics are driven by the wave-function probability density rather than the spatial phase of the wave function on the intermediate surface [2,3].

In this paper, we demonstrate how the spatially varying phase of the vibrational wave function can have a large influence on the dissociation of a molecule when a strong-field probe pulse mixes and reshapes the potential-energy surfaces of the molecule. We start with a general discussion of the surfaces and dynamics involved, and then proceed to the experimental measurements and detailed calculations which support our interpretation.

Figure 1 shows a cartoon of the essential states involved in the molecular dynamics. We impulsively launch a vibrational wave packet on the ground ionic state of the halomethane molecule CH_2XI (with X=Br or Cl) via strong-field ionization [4,5] in an intense ultrafast laser field [6,7]. The Keldysh parameter, γ, is approximately 0.7, indicating that the ionization has both tunnel and multiphoton character. The ionization produces a wave packet (initial launch position FC_{pump}) with significant displacement from its equilibrium position along the X-C-I bending coordinate. The displacement from equilibrium along other coordinates is substantially smaller (<0.006 Å for the bond lengths and <4% of the neutral equilibrium values for the other angles), and thus an essentially one-dimensional (1D) wave packet is launched in the ground state of the ion (V_0^{ion}). As the wave packet evolves in V_0^{ion}, near the minimum of the potential it comes into single-photon resonance (~1.58 eV) at FC_{probe} with an excited state of the ion that leads to dissociation (V_3^{ion}—the third excited ionic state for the molecules considered here). As FC_{probe} is near the center of V_0^{ion} the wave packet can be

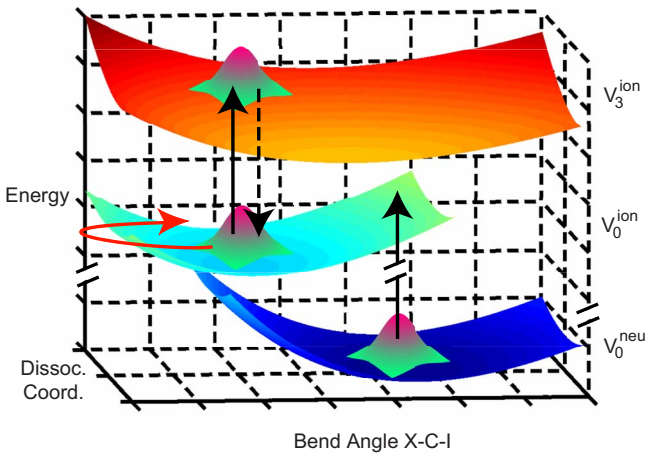


FIG. 1. (Color online) A cartoon of three important potential-energy surfaces in the CH_2XI family of molecules: the ground neutral state V_0^{neu}, the ground ionic state V_0^{ion} (reached via strong-field ionization—note the broken vertical axis), and an excited ionic state V_3^{ion}. A wave packet launched high on the latter surface can dissociate along the C-I bond.

*Corresponding author.

 ©2009 The American Physical Society

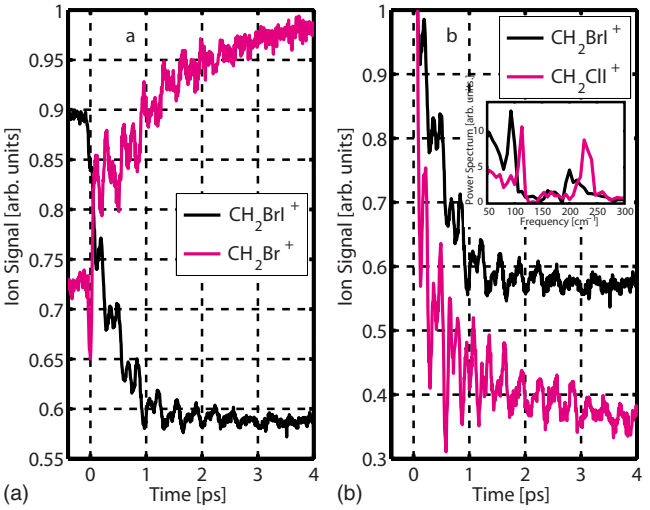


FIG. 2. (Color online) Pump-probe signals for several molecules. (a) CH_2BrI^+ and CH_2Br^+ from CH_2BrI. Note that the oscillations in the parent and daughter ions are perfectly π out of phase. (b) Two parent ions for comparison: CH_2BrI^+ and CH_2ClI^+. Inset: magnitude of the Fourier transforms for the data shown in panel (b).

promoted to V_3^{ion} twice per oscillation period if a probe pulse is incident on the molecule when the wave packet is at FC_{probe}. We find the transition probability for weak probe fields is the same regardless of the direction of wave-packet motion. However, for strong probe fields, we measure a significant difference in the bond-breaking probability that depends on the spatially varying phase (i.e., momentum) of the wave function in the ground ionic state and the strong-field coupling of the two potentials by the probe pulse.

II. EXPERIMENT

Our measurements begin with pulses from an amplified titanium:sapphire laser system (30 fs, 1 mJ) that are subsequently split in a Mach-Zehnder interferometer. One arm of the interferometer contains a pulse shaper with a computer-controlled acousto-optic modulator (AOM) as the shaping element [8]. The AOM can control the energy, duration, and chirp of either the pump or probe pulse. The two pulses are focused and intersect in an effusive molecular beam inside a vacuum chamber equipped with a time-of-flight mass spectrometer (TOFMS) that resolves the different fragment ions. Peak pump-pulse intensities are approximately 1.7×10^{14} W/cm^2, with typical pulse durations of 30–40 fs. For a more detailed description of the experimental apparatus see [9].

Pump-probe measurements in the CH_2XI family of molecules result in oscillating parent and daughter ion yields as a function of pump-probe delay, as seen in Fig. 2 for X=Br,Cl. The daughter ions that display modulations in their yield are all formed by the scission of a C-I bond: CH_2Br^+ from CH_2BrI and CH_2Cl^+ from CH_2ClI. As expected, the modulations in the daughter ion yields are always π out of phase with their respective parent ion [Fig. 2(a)]. A closer look at the parent ion signals [Fig. 2(b)] reveals that both CH_2BrI^+ and CH_2ClI^+ show oscillations at two frequencies.

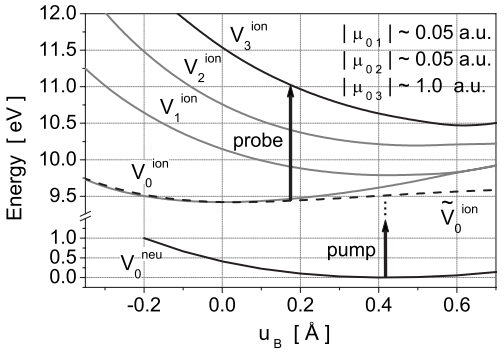


FIG. 3. Calculated potential-energy surfaces for CH_2BrI as a function of the bending normal coordinate u_B. The shading of the curves is roughly proportional to the strength of the transition dipole moment from V_0^{ion}. The dotted line indicates $\tilde{V}_0^{\text{ion}}$, the V_0^{ion} potential modified to emulate the effects of spin-orbit coupling.

In contrast, in symmetric molecules (CH_2I_2 and CH_2Br_2, not shown), the oscillations are only at a single frequency. The measurements for CH_2I_2 and CH_2Br_2 will be presented in a forthcoming publication. For the two-frequency oscillations, one frequency is the second harmonic of the other. Specifically, the frequencies are 94 ± 4 cm^{-1} and 196 ± 4 cm^{-1} for CH_2BrI^+, and 110 ± 4 cm^{-1} and 227 ± 4 cm^{-1} for CH_2ClI^+, as seen in the inset of Fig. 2(a). The fundamental frequencies match the I-C-X (X=Br,Cl) bending frequencies as measured and calculated in [10,11].

III. CALCULATIONS

Electronic structure and wave-packet propagation calculations are an essential part of interpreting our experimental results. We used the GAUSSIAN03 package of programs [12] and applied density-functional theory and time-dependent density-functional theory (TDDFT [13]) with the B3LYP functional [14] and the aug-cc-pVTZ-PP basis set [15] to calculate the equilibrium geometries, the normal-mode coordinates, and the relevant potential-energy curves for CH_2BrI. Details will be given in a forthcoming publication.

As the displacement of the ground state of the ion relative to the neutral equilibrium geometry is mostly along the I-C-Br bending normal coordinate u_B, we calculated the potential energies for the first four ionic states as a function of this coordinate. Figure 3 shows these states, along with the neutral ground state, as a function of u_B. The equilibrium I-C-Br angle for the CH_2BrI^+ cation is 95.5° (u_B=0 Å), while the equilibrium I-C-Br angle of the neutral CH_2BrI molecule in its ground electronic state is 114.9° (u_B=0.42 Å).

As discussed in the literature [10,11,16,17] there is a strong spin-orbit (SO) coupling between the ground and the first-excited ionic states of CH_2XI molecules. For CH_2BrI^+ this results in a bending vibrational frequency much lower than the 137 cm^{-1} obtained without SO coupling and produces a large anharmonicity (the measured vibrational frequencies for n=0, 7, and 8 are ν_0=116 cm^{-1}, 98.1 cm^{-1}, and 95.7 cm^{-1}, respectively [10].) In order to be consistent with these measurements without explicitly including SO

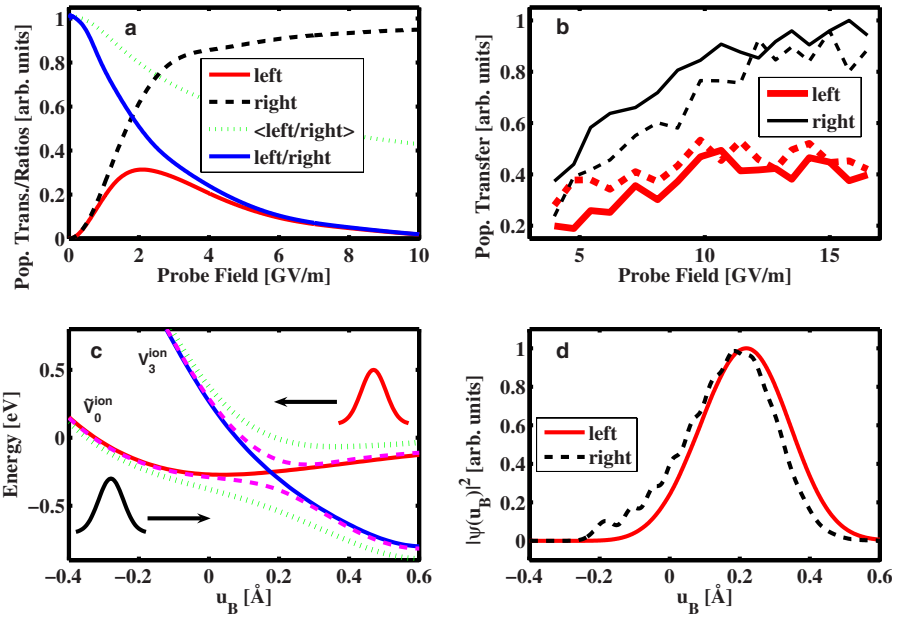


FIG. 4. (Color online) (a) The calculated population transferred from $\tilde{V}_0^{\text{ion}}$ to V_3^{ion} for left- (at 80 fs) and right-going (at 250 fs) wave packets as a function of peak field strength. Also shown are the calculated ratios of population transferred for left- and right-going wave packets as a function of field strength. The ratios are shown with (green dotted) and without (blue solid) volume and orientation averaging. (b) The experimental population transfer, measured as a depletion from the parent (depth of modulation in the oscillations). The thick red solid and dashed lines represent population transferred for two different left-going wave packets. The thin black lines represent population transferred for two different right-going wave packets. (c) Adiabatic dressed states calculated from $\tilde{V}_0^{\text{ion}}$ and V_3^{ion} in 2 GV/m (purple dashed lines) and 5 GV/m (green dotted lines) probe fields. Schematic wave packets are shown. (d) The calculated probability density for wave packets in $\tilde{V}_0^{\text{ion}}$ at 80 fs (left moving) and 250 fs (right moving).

coupling in our TDDFT calculations, we added a half-harmonic term to the V_0^{ion} (a^2A') potential to emulate the effect of the coupling to V_1^{ion} (a^2A'') on the shape of the ground ionic state and used the resulting $\tilde{V}_0^{\text{ion}}$ throughout the propagation. As the transition dipole moments (TDMs) computed between electronic states of different spatial symmetries are a factor of 20 lower than the TDM between V_0^{ion} and V_3^{ion} (see data in Fig. 3), only the electronic states V_0^{neu}, $\tilde{V}_0^{\text{ion}}$, and V_3^{ion} were considered in the simulations.

1D wave-packet propagations along u_B were performed using the split-operator method [18] together with the fast-Fourier technique [19]. The ground-state vibrational eigenfunctions were determined according to the Fourier-grid Hamiltonian method [20]. The interaction with the electric field (during wave-packet evolution on $\tilde{V}_0^{\text{ion}}$ and V_3^{ion}) was treated in the dipole approximation using the computed TDM between V_0^{ion} and V_3^{ion}, which turned out to be constant in the region near FC_{probe}. The ionization process was simulated by a single-photon resonant transition between V_0^{neu} and $\tilde{V}_0^{\text{ion}}$. Both the pump and probe pulses had $\sin^2(t)$ temporal intensity profiles with a full width at half maximum (FWHM) of 20 and 40 fs, respectively. The short pump pulse was chosen to mimic strong-field ionization near the peak of the pulse.

IV. DISCUSSION

The frequencies observed in CH_2BrI^+ do not match the frequencies of vibration near the potential minimum of the ground ionic state of the molecule. However, given the anharmonicity of the ground state of the ion, the 94 cm^{-1} modulations match the spacing between vibrational levels of the I-C-Br bending for states around $\nu=8$ [10]. In accordance with this, calculations and measurements of the FC factors for vertical ionization indicate that our pump pulse creates a wave packet in the ground state of the ion with a central vibrational quantum number of $\nu=7$ and a spread of roughly 6 to 8 states. This corresponds to a fairly localized wave packet (~0.2 Å FWHM) with a large displacement from equilibrium (~0.4 Å).

Figure 3 indicates that there is a resonance between $\tilde{V}_0^{\text{ion}}$ and V_3^{ion} at $u_B \sim 0.18$ Å in the I-C-Br bending mode (~104°). The resonance location being near (but not at) the center of $\tilde{V}_0^{\text{ion}}$ leads naturally to the presence of both the 94 cm^{-1} and 196 cm^{-1} modulations as the wave packet can be promoted to the final state twice per oscillation period. Calculations of the population transfer versus pump-probe delay yield modulations containing both frequencies. Once the wave packet is promoted to V_3^{ion} it is energetically possible to dissociate, and bond-order analysis similar to [21,22] indicates that C-I scission is likely from this state, consistent with previous dissociative photoionization experiments [23].

In the limit of weak coupling between $\tilde{V}_0^{\text{ion}}$ and V_3^{ion} by the probe pulse, our calculations indicate that the amount of wave packet transferred is independent of the wave-packet momentum since the wave packet has almost exactly the same probability distribution at the resonance location moving to smaller angles (to the left) as moving to larger ones [to

the right; see Fig. 4(d)]. However, both measurements and calculations indicate that for strong couplings, there is an asymmetry in the population transfer for the two different wave-packet momenta. For high intensities, the molecule can become completely transparent to the probe pulse for a left-going wave packet, leading to negligible dissociation. This is shown in Fig. 4(a), which plots the calculated population transferred to V_3^{ion} from $\tilde{V}_0^{\text{ion}}$ as a function of probe pulse field strength for two delay times that correspond to a left- and right-going wave packet at the resonance location. Also, shown is the ratio of the left- and right-going population transfer as a function of probe field strength.

Our experimental measurements of the population transfer to V_3^{ion} as a function of probe pulse field strength are shown in Fig. 4(b), which plots the depletion in the parent ion signal (depth of modulation in the oscillations) for delay times corresponding to left- and right-going wave packets at the resonance location. These measurements indicate that the dissociation for left- and right-going wave packets is roughly symmetric for weak coupling between the potentials (weak probe pulse field) but different for strong coupling (strong probe pulse field). Intensity volume and angle averaging in the experiment (collection of molecular ions which are exposed to different probe pulse intensities in the transverse profile of probe beam and different projections of the molecular transition dipole moments on the probe pulse polarization axis) keeps the population transfer for a left-going wave packet from returning to zero for high probe pulse energies. Calculations which roughly model the intensity volume and orientation averaging using a weighted average of population transfer calculated for different probe intensities and angles between the TDM and laser polarization vector are shown in Fig. 4(a). The dotted green curve and the solid blue curve show the ratio of the population transfer for left- and right-going wave packets with and without the intensity volume and orientation averaging, respectively. The calculated right/left ratio at 10 GV/m is about 2, which is in agreement with our experimental measurements.

As the calculations and measurements indicate that the asymmetry in the bond breaking is a strong-field effect, we turn to a dressed-state picture to interpret the dynamics. Figure 4(c) shows the dressed states near the resonance between $\tilde{V}_0^{\text{ion}}$ and V_3^{ion} when coupled by the resonant probe pulse (V_3^{ion} shifted downwards by $h\nu=1.58$ eV). At low probe pulse field strengths, the adiabatic curves (purple dashed curves) lie close together, and the probability for the wave packet to jump between adiabatic states (i.e., nonadiabatic passage) is significant as the wave packet traverses the avoided crossing in either direction. Thus, via a combination of adiabatic and nonadiabatic passage, there is some population transfer (within the ~40 fs probe pulse duration) with low probe field strengths for both left- and right-going wave packets.

In the case of a strong probe pulse field, the dressed states (green dotted curves) are well separated and the wave packet adiabatically follows them. The left-going wave packet enters on the upper adiabatic state, and turns around before passing through the avoided crossing. It therefore stays on $\tilde{V}_0^{\text{ion}}$ and does not dissociate. The right-going wave packet enters on the lower adiabatic potential and does not return to the avoided crossing while the probe pulse is on. As the character of the dressed states changes in passing through the avoided crossing, the wave packet finds itself on V_3^{ion} after passing through the avoided crossing once on the lower adiabatic state.

Note that while our results are somewhat similar to [2,3], those results relied on the wave function having different amplitudes when moving left and right. In our case, as shown in Fig. 4(d), the amplitudes are nearly identical for left- and right-going wave packets on the $\tilde{V}_0^{\text{ion}}$ potential of CH_2BrI. It is the combination of the spatially varying phase and distortion of the molecular potentials by the laser field that lead to the asymmetry in our measured dissociation yield. The dynamics here are similar to those responsible for "molecular bond locking," as discussed in [24]. However, since $\tilde{V}_0^{\text{ion}}$ is not as steep as V_3^{ion} in the vicinity of the resonance, the wave packet is not locked in position, but rather trapped on $\tilde{V}_0^{\text{ion}}$ when it is moving left and completely transferred between $\tilde{V}_0^{\text{ion}}$ and V_3^{ion} when going right.

V. CONCLUSION

In conclusion, we have shown how the spatially varying phase (or momentum) of a wave packet can have a dramatic effect on the dissociation of a molecule on light-dressed potential-energy surfaces. A probe pulse following the launch of the wave packet by a strong-field pump pulse can be used to switch the wave packet from a bound state to a dissociative one, with the wave-packet momentum and probe field strength determining the switching probability.

ACKNOWLEDGMENTS

We gratefully acknowledge support from the National Science Foundation under Award No. 0555214 and support from the Hungarian Academy of Sciences and the Deutsche Forschungsgemeinschaft (DFG) under Grant No. 436 UNG 113/188/0-1, as well as fruitful discussions with Professor Leticia González, Dr. Jesús González Vázquez, and Professor István Mayer.

[1] A. H. Zewail, *Femtochemistry—Ultrafast Dynamics of The Chemical Bond* (World Scientific, Singapore, 1994), Vols. 1 and 2.

[2] P. Cong, G. Roberts, J. L. Herek, A. Mohktari, and A. H. Zewail, J. Phys. Chem. **100**, 7832 (1996).

[3] B. Kohler, V. V. Yakovlev, J. Che, J. L. Krause, M. Messina, K. R. Wilson, N. Schwentner, R. M. Whitnell, and Y. J. Yan, Phys. Rev. Lett. **74**, 3360 (1995).

[4] M. V. Ammosov, N. B. Delone, and V. P. Krainov, Zh. Eksp. Teor. Fiz. **91**, 2008 (1986) [Sov. Phys. JETP **64**, 1191 (1986)].
[5] X. M. Tong, Z. X. Zhao, and C. D. Lin, Phys. Rev. A **66**, 033402 (2002).
[6] B. J. Pearson, S. R. Nichols, and T. C. Weinacht, J. Chem. Phys. **127**, 131101 (2007).
[7] Z. H. Loh and S. R. Leone, J. Chem. Phys. **128**, 204302 (2008).
[8] M. A. Dugan, J. X. Tull, and W. S. Warren, J. Opt. Soc. Am. B **14**, 2348 (1997).
[9] F. Langhojer, D. Cardoza, M. Baertschy, and T. Weinacht, J. Chem. Phys. **122**, 014102 (2005).
[10] M. Lee, H. Kim, Y. S. Lee, and M. S. Kim, J. Chem. Phys. **122**, 244319 (2005).
[11] M. Lee, H. Kim, Y. S. Lee, and M. S. Kim, J. Chem. Phys. **123**, 024310 (2005).
[12] M. J. Frisch, G. W. Trucks, H. B. Schlegel, G. E. Scuseria, M. A. Robb, J. R. Cheeseman, J. A. Montgomery, Jr., T. Vreven, K. N. Kudin, J. C. Burant, J. M. Millam, S. S. Iyengar, J. Tomasi, V. Barone, B. Mennucci, M. Cossi, G. Scalmani, N. Rega, G. A. Petersson, H. Nakatsuji, M. Hada, M. Ehara, K. Toyota, R. Fukuda, J. Hasegawa, M. Ishida, T. Nakajima, Y. Honda, O. Kitao, H. Nakai, M. Klene, X. Li, J. E. Knox, H. P. Hratchian, J. B. Cross, C. Adamo, J. Jaramillo, R. Gomperts, R. E. Stratmann, O. Yazyev, A. J. Austin, R. Cammi, C. Pomelli, J. W. Ochterski, P. Y. Ayala, K. Morokuma, G. A. Voth, P. Salvador, J. J. Dannenberg, V. G. Zakrzewski, S. Dapprich, A. D. Daniels, M. C. Strain, O. Farkas, D. K. Malick, A. D. Rabuck, K. Raghavachari, J. B. Foresman, J. V. Ortiz, Q. Cui, A. G. Baboul, S. Clifford, J. Cioslowski, B. B. Stefanov, G. Liu, A. Liashenko, P. Piskorz, I. Komaromi, R. L. Martin, D. J. Fox, T. Keith, M. A. Al-Laham, C. Y. Peng, A. Nanayakkara, M. Challacombe, P. M. W. Gill, B. Johnson, W. Chen, M. W. Wong, C. Gonzalez, and J. A. Pople, *GAUSSIAN 2003*, Gaussian Inc., Wallingford, CT, 2003.
[13] M. Casida, *Recent Advances in Density Functional Methods, Part I* (World Scientific, Singapore, 1995).
[14] P. J. Stephens, F. J. Devlin, C. F. Chabalowski, and M. J. Frisch, J. Phys. Chem. **98**, 11623 (1994).
[15] K. Peterson,D. Figgen, E. Goll, H. Stoll, and M. Dolg, J. Chem. Phys. **119**, 11113 (2003).
[16] M. Lee and M. S. Kim, Chem. Phys. Lett. **431**, 19 (2006).
[17] M. Lee, H. Kim, Y. S. Lee, and M. S. Kim, Angew. Chem. Int. Ed. **44**, 2929 (2005).
[18] M. D. Feit, J. A. Fleck, and A. Steiger, J. Comput. Phys. **47**, 412 (1982).
[19] D. Kosloff and R. Kosloff, J. Comput. Phys. **52**, 35 (1983).
[20] C. Marston and G. Balint-Kurti, J. Chem. Phys. **91**, 3571 (1989).
[21] I. Mayer and A. Gömöry, Chem. Phys. Lett. **344**, 553 (2001).
[22] I. Mayer and A. Hamza, Program "APOST," Version 1.09, 2004, (http://occam.chemres.hu/programs).
[23] A. F. Lago, J. P. Kercher, A. Bödi, B. Sztáray, B. Miller, D. Wurzelmann, and T. Baer, J. Phys. Chem. A **109**, 1802 (2005).
[24] T. Szakács, B. Amstrup, P. Gross, R. Kosloff, H. Rabitz, and A. Lörincz, Phys. Rev. A **50**, 2540 (1994).